

# **UNCERTAINTY QUANTIFICATION OF CALCULATED FUEL TEMPERATURE FOR AGR-3/4 IRRADIATION EXPERIMENT**

B.T. Pham, N.J. Nancy, G.H. Hawkes,  
J.J. Einerson

September 2018



The INL is a U.S. Department of Energy National Laboratory  
operated by Battelle Energy Alliance

# **UNCERTAINTY QUANTIFICATION OF CALCULATED FUEL TEMPERATURE FOR AGR-3/4 IRRADIATION EXPERIMENT**

**B.T. Pham, N.J. Nancy, G.H. Hawkes, J.J. Einerson**

**September 2018**

**Idaho National Laboratory  
Idaho Falls, Idaho 83415**

**<http://www.inl.gov>**

**Prepared for the  
U.S. Department of Energy**

**Under DOE Idaho Operations Office  
Contract DE-AC07-05ID14517**

## UNCERTAINTY QUANTIFICATION OF CALCULATED FUEL TEMPERATURE FOR THE AGR-3/4 IRRADIATION EXPERIMENT

**B.T. Pham<sup>1</sup>, N.J. Lybeck<sup>1</sup>, G.L. Hawkes<sup>1</sup>, J.J. Einerson<sup>1</sup>**

<sup>1</sup>Idaho National Laboratory, 2525 N Fremont Ave, Idaho Falls, ID 83415, USA

Binh.Pham@inl.gov, Nancy.Lybeck@inl.gov, Grant.Hawkes@inl.gov, EinersonJeff@gmail.com

### ABSTRACT

The third in a series of Advanced Gas Reactor (AGR) experiments conducted at the Idaho National Laboratory, AGR-3/4, was completed in April 2014, resulting in irradiation of the tristructural isotropic fuel for 369 effective full-power days. A number of designed-to-fail fuel particles were embedded along the central line of each irradiated compact to provide a known source of fission products for subsequent transport through the compact matrix and structural graphite materials. The fuel temperature in each capsule during irradiation, a significant factor in the release and transport of fission products, was maintained within a predefined range representative of a high-temperature gas reactor. Fuel temperatures were not measured directly because contact between a thermocouple and the fuel could lead to unwanted particle failures. An ABAQUS-based finite element heat transfer code, calibrated based on temperatures measured in the surrounding graphite rings, was used to predict fuel temperatures during irradiation.

To quantify the uncertainty of calculated fuel temperatures, thermal model parameters with high sensitivity and/or large uncertainty were identified. Propagation of model parameter uncertainty and sensitivity is then used to quantify the overall uncertainty of calculated temperatures. Quantification of input uncertainties over the extended irradiation period of the AGR-3/4 experiment is a challenging task due to changes in capsule thermal properties and geometry caused by exposure to neutron irradiation at high temperatures. In the absence of direct measurements or complete knowledge about these changes, inputs to the thermal model and associated uncertainties are estimated based on modeling assumptions and expert judgment. Unplanned events that occurred during irradiation contribute to input uncertainties as well. For example, shrinkage of the fuel compact and graphite rings led to a significant increase in the gap-size uncertainties. This paper focuses on uncertainty quantification of calculated fuel temperature for AGR-3/4 capsule thermal models.

### 1. INTRODUCTION

The third in a series of Advanced Gas Reactor (AGR) experiments conducted at the Idaho National Laboratory (INL), AGR-3/4, was completed in April 2014, resulting in irradiation of the tristructural isotropic (TRISO) fuel for 369 effective full-power days. The main objectives of these tests are to provide the necessary data on fuel performance to support qualification of the fuel design and fabrication process for normal operation and postulated accident conditions, and support development and validation of fuel performance and fission-product transport models

and codes [1]. The AGR-3/4 test consists of twelve independent capsules containing TRISO uranium oxy-carbide fuel particles embedded in four cylindrical compacts stacked on top of each other. A number of designed-to-fail fuel particles were embedded along the central line of each irradiated compact to provide a known source of fission products for subsequent transport through the compact matrix and structural graphite materials [2].

The experiment was designed to maintain fuel temperatures, which affect release and transport of fission products, within a predefined range representative of a high-temperature gas reactor. Fuel temperatures were not measured directly because contact between a thermocouple (TC) and the fuel could lead to unwanted particle failures. A Monte Carlo depletion analysis was performed using JMOCUP [3] to calculate fast fluence and fission heat rate data for the fuel compacts, graphite rings, and stainless steel capsule shell, which are required inputs for the finite element heat transfer code used to predict fuel temperatures during irradiation [4]. The thermal model was calibrated based on temperatures measured in the surrounding graphite rings, and incorporates complex physical mechanisms and properties changing with fast-neutron fluence such as graphite-ring and fuel-compact shrinkage, conductivity, and density.

The predicted temperatures are affected by uncertainty in input parameters and by modeling assumptions made due to incomplete knowledge of the underlying physics. Therefore, along with the deterministic predictions from a set of input thermal conditions, information about prediction uncertainty is instrumental for interpretation of the experimental results. Well defined and reduced uncertainty in model predictions helps increase the quality of and confidence in AGR technical findings [5]. A process for quantifying uncertainty in the calculated fuel temperatures for the AGR fuel irradiation experiments is presented in [6]. This paper focuses on temperature uncertainty quantification for the AGR-3/4 experiment.

## **2. AGR-3/4 CAPSULE THERMAL MODELS**

The AGR-3/4 test train was irradiated in the northeast flux trap of the Advanced Test Reactor (ATR) at INL. Reactor coolant water flowed on the outside of each stainless steel capsule shell. Every capsule has a stack of four fuel compacts in the center surrounded by three graphitic annuli; proceeding from the compact out are the inner ring, the outer ring, and the graphite sink, which are housed in a stainless steel capsule shell (Figure 1). This design features four gaps that are filled with gas in order to control temperature: Gas Gap 1, between the fuel stack and the inner surface of the inner ring; Gas Gap 2, between the inner ring and the inner surface of the outer ring; Gas Gap 3, between the outer ring and the inner surface of the graphite sink; and Gas Gap 4, between the graphite sink and the inner surface of the capsule shell. By design, Gas Gaps 1 and 2 are small, minimizing the temperature difference between inner and outer rings.

Each capsule is instrumented with two or three TCs embedded in the graphite rings and an independent gas line to route a mixture of helium and neon gases through the gas gaps, enabling temperature control. The predefined target TC temperature is used as a feedback for the gas-flow controller to deliver the necessary neon/helium gas mixture (between 100% helium for high conductivity and 100% neon for low conductivity) to maintain desired fuel temperatures in response to variations in the ATR power [2]. Gas-flow rates in each capsule were maintained around 30 standard cubic centimeters per minute (sccm) for pressures in the approximate range 1–3 psig.

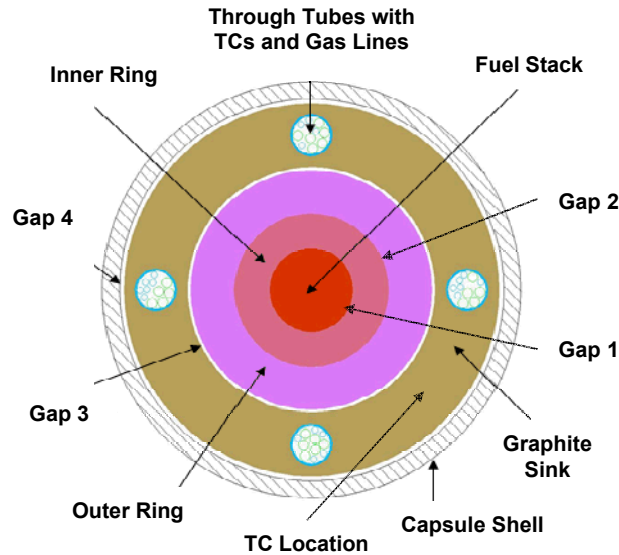


Figure 1 – Schematic of radial cut of AGR-3/4 capsule.

One ABAQUS-based (Version 6.14 2), three-dimensional finite element thermal model is created for each capsule to predict daily average temperatures of fuel compacts and at TC locations during irradiation. The thermal model uses a high-resolution mesh composed of approximately 400,000 8-node hexahedral brick elements to estimate capsule temperature profiles, as shown in Figure 2. A basic mesh was created for one capsule and then was propagated to other capsules by varying gas-gap conductivity (and, hence, gap conductance) to compensate for individual capsule gap dimensions and changes in the gap size during irradiation. The model details, including model validation and verification, calibration, sensitivity analysis, and results are described in [4].

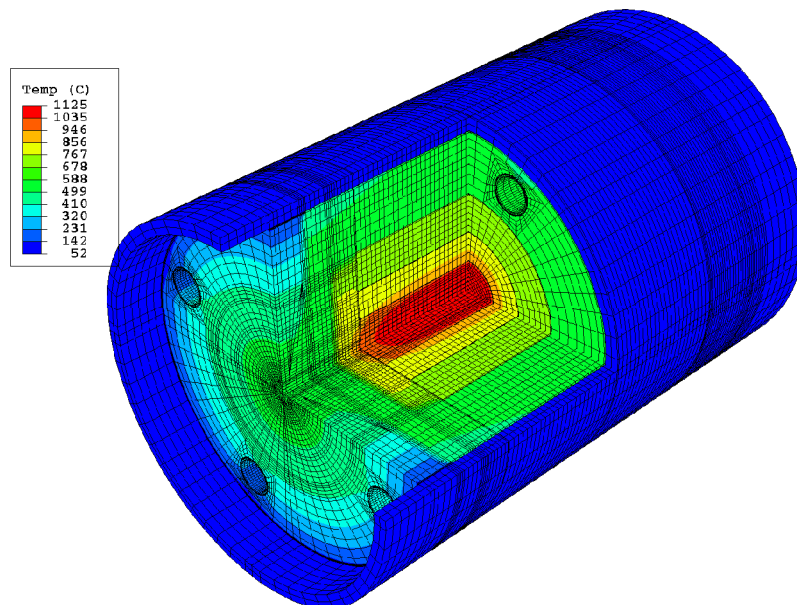


Figure 2 – Cutaway view of finite element of AGR-3/4 capsule.

Fission power generated in the fuel compacts and three graphite rings is primarily conducted and radiated out through the four gas gaps to the ATR primary cooling water, which serves as the ultimate heat sink for all capsules. The governing equations of steady-state conduction and radiation heat transfer are used for the thermal models. An adiabatic boundary condition was placed on the top and bottom of each capsule. A heat-transfer coefficient connected to the cooling water was placed on the outside of the capsule shell. The measured cooling water temperature is within 0.5°C of the calculated temperatures, indicating good model performance. To reduce the calculated temperature uncertainty, rigorous calibration was performed to get a better match with TC readings over the extended course of irradiation, and dimensional measurements obtained during the AGR-3/4 post-irradiation examination are used to establish variable gas-gap models, reducing gas-gap uncertainties [8].

### 3. UNCERTAINTY QUANTIFICATION OF CALCULATED FUEL TEMPERATURE

Assuming numerical errors are minimized by using sufficient resolution of the finite element mesh in the computing code, uncertainty in the prediction of a simulation model arises from two main sources: input uncertainty and model form uncertainty (bias). Subsequently, the overall uncertainty of simulation model predictions can be expressed in terms of variance as:

$$\sigma_T^2 = \sigma_P^2 + \sigma_B^2 \quad (1)$$

where  $\sigma_T^2$ ,  $\sigma_P^2$ , and  $\sigma_B^2$  represent the uncertainty of calculated temperature, input uncertainty, and model form uncertainty, respectively. The following sections describe the uncertainty quantification results for the AGR-3/4 fuel temperatures.

#### 3.1 Model Form Uncertainty

Model form uncertainty or bias represents consistent differences between predicted and measured temperatures resulting from lack of knowledge of the underlying physics in the capsule thermal processes. Because TCs are susceptible to drift failures caused by extended exposure to high temperatures and fast-neutron irradiation, an analysis was performed to verify that the AGR-3/4 TCs operated reliably, especially during the earlier cycles of irradiation. Therefore, TC residuals (measured minus calculated temperatures) at each time step (each day) can be used to assess model bias. The relative model uncertainty for calculated temperature can then be calculated as the ratio between the average TC residual and the average TC temperature. Temperature data from the first three ATR cycles were used to determine the model biases presented in Table 1. Capsules 5, 7, 9, and 10 have insignificant model bias (<1% in absolute value), indicating an excellent fit between measured and calculated TC temperatures and offering confidence that the thermal model has appropriately incorporated all important physical phenomena occurring in the capsule. Model biases for the remaining capsules are moderate (<5% in absolute value), with the exception that Capsule 11 has the largest relative model bias of -9.9%.

Table 1 - Thermal model biases for 12 AGR-3/4 capsules.

Capsule	1	2	3	4	5	6	7	8	9	10	11	12
Model Bias, %	3.6	1.4	2.0	1.4	0.5	1.9	0.6	2.4	0.1	-0.6	-9.9	-4.7

### 3.2 Input Parameter Uncertainty

The input uncertainty of a calculated temperature is a result of uncertainties in the input parameters to the thermal model. To quantify this uncertainty, model inputs of potential importance to temperature are identified in a two-part process: (1) using sensitivity analysis to determine which parameters the model is most sensitive to, and (2) using expert judgment to determine which input parameters have the largest uncertainties and estimate these uncertainties. A subset of the input parameters is then selected for calculated temperature-uncertainty quantification, including those with high sensitivity and those with large uncertainty. Forward uncertainty propagation based on input uncertainties and sensitivity coefficients is used to calculate the input uncertainty of the calculated temperatures by assuming that the calculated temperature can be approximated by a weighted sum of the input parameters [6]:

$$\sigma_P^2 = \sum_i^n a_i^2 \sigma_i^2 + \sum_i^n \sum_{j \neq i}^n \rho_{ij} a_i \sigma_i a_j \sigma_j \quad (2)$$

where  $a_i^2$  is the square of the sensitivity coefficient for parameter  $i$ ,  $\sigma_i^2$  is uncertainty of input parameter  $i$  in terms of variance,  $\rho_{ij}$  is the correlation coefficient for input parameters  $i$  and  $j$ , and  $n$  is the number of input parameters.

#### 3.2.1 Sensitivity analysis

Parameter sensitivity quantifies the influence of an input parameter on calculated temperatures. A first-order sensitivity evaluation for the temperature calculations was performed for one AGR-3/4 capsule at one time step during the first ATR cycle [7]. A series of cases were compared to a nominal case by varying different input parameters into the capsule thermal model in order to evaluate the temperature sensitivity to each parameter. The tornado plot in Figure 3 shows the sensitivities of input parameters on fuel temperature as changes in fuel temperature when each input was changed by  $\pm 10\%$  (numbers on the y-axis), sorted from largest to smallest. The most sensitive parameter was the compact heat rate, followed by the neon gas fraction. Three gap distances (1, 3, and 4), component and graphite (sink) heat rates, and thermal conductivity of the compacts and the graphite rings all exhibit moderate sensitivity. The least sensitive parameters were the emissivity of the stainless steel and graphite, along with Gap 2 distance.

For fuel temperature uncertainty quantification, the sensitivity analysis performed went beyond the traditional local sensitivity. To establish sufficiency of the first-order (linear) expansion terms in constructing the temperature-response surface, analysis of pairwise interactions of model parameters was also performed using experimental design to select a minimum number of necessary simulation runs. Furthermore, using an interpolation scheme over the input parameter domain, the analysis obtains time-dependent sensitivity over the test-campaign duration. This allows computation of uncertainty for the calculated fuel temperatures for all time steps over the entire irradiation period [6].

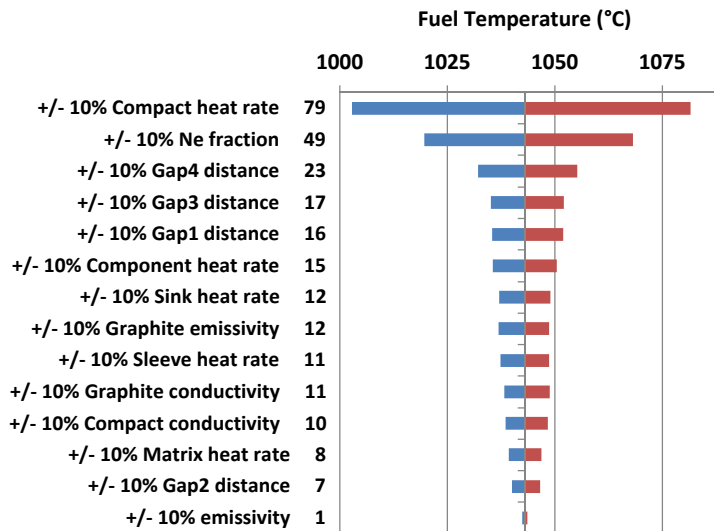


Figure 3 – Input sensitivities of fuel temperatures in one AGR-3/4 capsule.

### 3.2.2 Input uncertainty analysis

The range of uncertainties for identified inputs to the thermal model is determined by AGR campaign experts. Expert judgment takes into account machining tolerances for capsule geometry, measurement uncertainty of mass-flow controllers, model uncertainty of depletion analysis results, and legacy experience for fuel-compact and graphite conductivity and emissivity. Relative uncertainties of main inputs to the thermal model, expressed in the range of percent of input value (%), are presented in Table 2 for the AGR-3/4 capsules.

Table 2 – Uncertainties of main inputs to the thermal model of the AGR-3/4 capsules.

Parameter	Uncertainty	Rationale
Gas Gap 1 (~0.075 mm)	10–40%	Gas gap size uncertainty sources are: <ul style="list-style-type: none"> <li>0.0254-mm uncertainty at the start of irradiation due to fabrication tolerances</li> <li>Post-irradiation examination (PIE) metrology uncertainties are used at the end of irradiation</li> <li>20% uncertainty in the graphite thermal expansion coefficient results in additional 0.006-mm uncertainties for all time steps.</li> </ul>
Gas Gap 2 (0.07–1.2 mm)	5–50%	
Gas Gap 3 (0.08–3.8 mm)	1–40%	
Gas Gap 4 (0.38–2.3 mm)	2–10%	
Neon fraction	3–30%	Uncertainty is based on 1-sccm flow rate tolerance.
Fuel-compact heat rate	5%	Based on good agreement between measured and calculated burnup of the AGR-1 compacts.
Graphite-ring heat rate	3%	
Graphite conductivity	15%	Additional conductivity data for the test graphite allows a lower uncertainty estimate for graphite than for fuel compacts.
Fuel-compact conductivity	20%	Uncertainty is based on work done on surrogate compacts by C. Folsom at Utah State University.



Uncertainties of the four gas-gap distances vary over time due to gradual irradiation-induced changes in capsule geometry, as described in detail in [8]. Uncertainty of the neon fraction, which is used to determine gas-gap conductivity, also varies with time, and is in the range of 3–30% depending on the actual fraction value. The main source of neon fraction uncertainty is measurement error in the gas-flow meters, which have a 1 sccm tolerance based on engineering assessment; hence, higher relative uncertainty was estimated at lower neon fractions [6].

The remaining input uncertainties are assumed to be constant for all time steps due to lack of experimental data directly relevant to AGR-3/4 capsules. The uncertainty in heat rate is caused by a combination of several factors from measured data input parameters that go into the physics calculation and Monte Carlo statistical uncertainties associated with calculated parameters. Low uncertainties for fuel and graphite heat rates (5% and 3%, respectively) are justifiable because of respectable agreement between burnup measured during PIE and calculated by the physics model for AGR-1 compacts, indicating excellent predictability [9]. Graphite heating is primarily caused by ATR-core neutron and gamma radiation interaction; equations used to calculate heat rates are relatively accurate and directly scalable to ATR core power, resulting in lower uncertainty in the graphite heat rate. Finally, thermal conductivities for the fuel compacts and graphite rings were extrapolated from correlations based on data from legacy experiments, resulting in higher uncertainties. This leads to high uncertainties of fuel compact and graphite conductivities. Uncertainty in thermal conductivity for the graphite rings is assessed to be lower than for the fuel compacts because there was a more relevant data point available for validation of the graphite correlation.

### ***3.2.3 Input selection for temperature uncertainty quantification***

Based on results of sensitivity and uncertainty analysis, nine influential inputs were selected for evaluation in the uncertainty quantification of AGR-3/4 calculated fuel temperatures:

- Compact heat rate (highest sensitivity)
- Neon fraction of the gas mixture due (high sensitivity and wide uncertainty range)
- Gas Gaps 1–4 (moderate sensitivity [except Gas Gap 2] and wide uncertainty range)
- Compact and graphite-ring thermal conductivities (high uncertainty)
- Graphite heat rate (moderate sensitivity and low uncertainty).

### ***3.2.4 Correlation coefficients***

Among the nine selected inputs, the fuel-compact and graphite heat rates are directly defined by fast-neutron fluence; therefore, their correlation coefficient should be very high, and is conservatively assumed to be one. The correlation coefficients between fuel compact and graphite conductivities are also expected to be high because both are calculated from similar correlations of temperature and fast-neutron fluence. These correlation coefficients for AGR-3/4 capsules are in a range of 0.5–0.95 as a function of fast fluence, as described in [6]. For the remaining input pairs, the correlation coefficients are deemed negligible because the input acquisition processes are independent (e.g., gas-gap distances were measured and heat rates were calculated).

### 3.2.5 Propagation of input uncertainties through sensitivities

The uncertainties and sensitivity coefficients for nine selected inputs are estimated for each time step and each capsule over the entire irradiation campaign. Relative input uncertainties in terms of one standard deviation (%) are used to quantify the overall calculated temperature uncertainty. Variance of fuel temperature caused by uncertainty in a specific input parameter is defined as the square of uncertainty weighted by the square of the sensitivity coefficient. The primary contribution of each individual parameter to the parameter uncertainty of the calculated temperatures in Eq. 2 can be assessed based on the temperature variance caused by parameter uncertainty.

Figure 4 shows daily input uncertainty, input sensitivity of fuel temperature, variance of fuel temperature due to each input uncertainty, and resulting uncertainty of fuel temperature as a function of effective full-power days of irradiation for Capsule 9. These plots vary somewhat for other capsules due to differences in thermal conditions, but the data trends are similar. The following primary results of propagation of input uncertainties to calculated temperature uncertainty are observed:

*Input uncertainty (Frame 1):* Relative uncertainties for the four gas gaps and neon fraction vary with irradiation time. The highest input uncertainty at the beginning of irradiation is Gas Gap 1 (light-green line) and at the end of irradiation is Gas Gap 3 (cyan line). Gas Gap 1 uncertainty is decreasing with time due to an increase in the gap distance as irradiation progresses. The opposite was observed for Gas Gap 3 because this gap distance decreases with irradiation time. The relative uncertainty of Gas Gap 4 is low (~5%) due to its larger gap sizes. Neon fraction uncertainties (green line) are mainly in the range of 3–6% due to typically high neon fractions in this capsule. Neon-fraction uncertainties are higher for time steps at the beginning of each cycle when the neon fraction was low. Uncertainties for the remaining inputs are unchanged with irradiation time, as indicated by flat lines.

*Input sensitivity (Frame 2):* The sensitivities of fuel temperatures to some inputs vary with time, reflecting the inherent non-linearity of the thermal models as a result of complex interactions between simultaneously changing inputs. The fuel heat rate (red line) has the highest sensitivity for fuel temperature (~ 0.4) followed by the neon fraction, Gas Gap 4, and the graphite heat rate (green, black, and blue lines, respectively), as expected from the tornado plot in Figure 3. The sensitivities to the fuel and graphite conductivities are negative and flat.

*Variance due to changes in individual inputs (Frame 3):* The temperature variances in response to variations of input uncertainty and sensitivity also change over time. Moderate sensitivity, combined with high uncertainty of graphite thermal conductivity, (orange line) made it the dominant factor for fuel-temperature uncertainty during most of the irradiation, except for the first 40 days. During these days, Gas Gap 1, located next to fuel compacts, is the dominant factor due to higher uncertainty (light-green line). Fuel heat rate (red line), which has the highest sensitivity and relatively low uncertainty, is the second dominant factor for fuel temperature uncertainty behind graphite conductivity. Uncertainties of neon fraction, graphite heat rate, and Gas Gaps 2–4 have minor impact on uncertainty of fuel temperature because of low temperature variances.

*Input parameter uncertainty of fuel temperature (Frame 4):* The resulting input uncertainties of fuel temperature are in the range of 3.6–4.4% over the course of the experiment. The decrease in temperature parameter uncertainty with time was driven by the decrease in temperature variance

due to Gas Gap 1 uncertainty (light-green line in Frame 3) as variances caused by other inputs remain fairly constant. This shows the large impact Gas Gap 1 has on uncertainty of fuel temperature, especially at the beginning of irradiation.

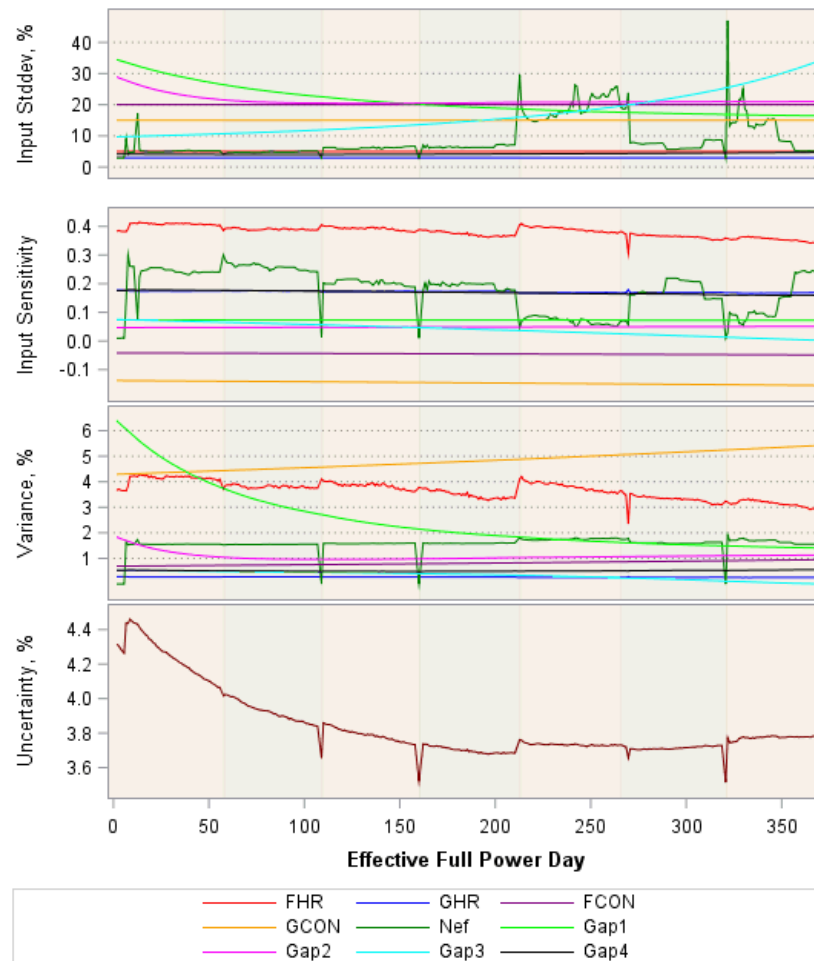


Figure 4 – History of input uncertainty, sensitivity, variance, and uncertainty of fuel temperature.

### 3.3 Uncertainty of Calculated Fuel Temperature

Overall uncertainty of fuel temperature in terms of variance equals the total of model form uncertainty and parameter uncertainty as expressed in Eq. 1. For each capsule, the uncertainty quantification of fuel temperature was performed for all time steps. Figure 5 depicts calculated fuel temperatures (solid lines) and a one standard deviation uncertainty band (shaded areas) as a function of effective full-power days of irradiation for the AGR-3/4 capsules. The drops in fuel temperatures occurred at the start of each ATR fuel cycle when the reactor was powering up. Notably, the uncertainty bands have similar widths for all capsules, except for Capsule 11, which shows a significantly larger uncertainty band (the purple-shaded area). This remarkably large fuel temperature uncertainty in Capsule 11 is caused by a higher modeling bias of -9.9% (Table 1), indicating the thermal model consistently over predicts temperatures at TC locations in this capsule.

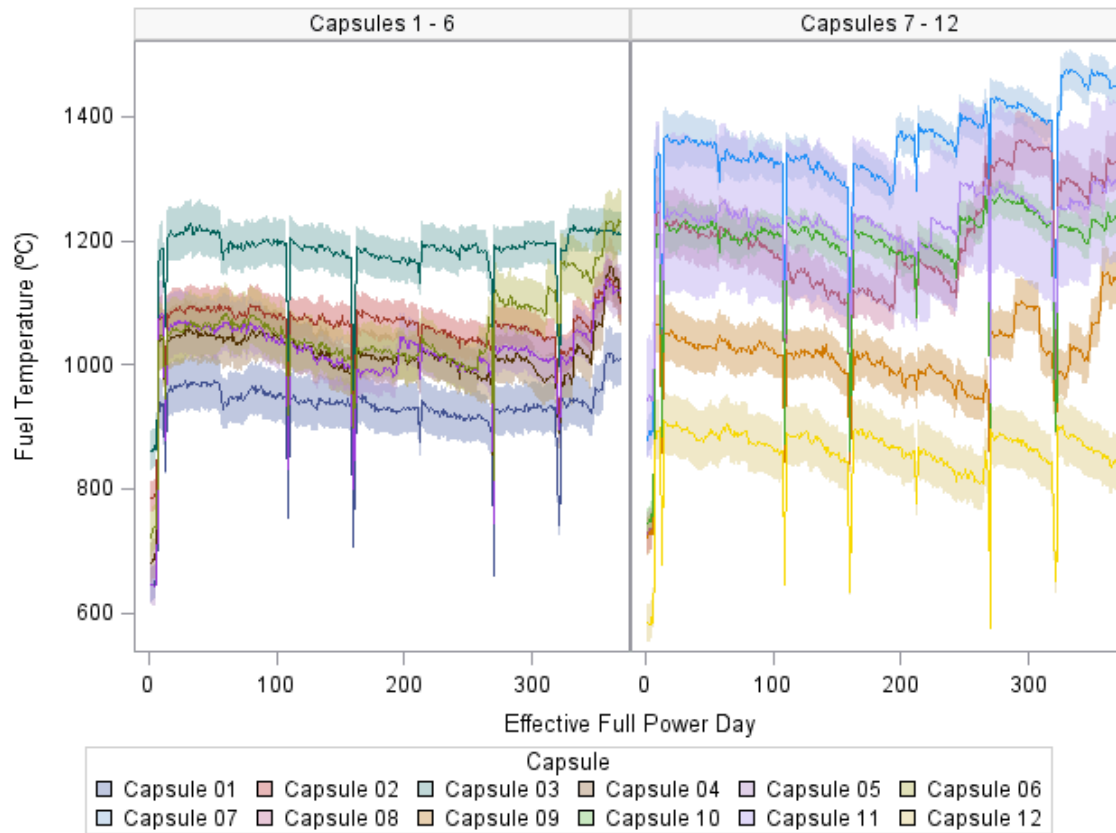


Figure 5 – Calculated fuel temperature with uncertainty in AGR-3/4 capsules.

The average fuel temperature uncertainties in terms of one relative and absolute standard deviation are summarized in Table 3 for the twelve capsules. Capsules 2, 7, and 10 temperatures have the lowest uncertainty, just over 30°C (or ~3%), because of their negligible model bias and low uncertainties of the four gap sizes. Capsules 3 and 9 have slightly higher temperature uncertainty due to higher model bias in Capsule 3 and higher gap-size uncertainties in Capsule 9. Capsule 11 temperature uncertainties are 125°C on average (or 10.1%). The six remaining capsules have temperature uncertainties between 40–46°C (3.8–5.3%).

Table 3. Calculated fuel temperature uncertainties for AGR-3/4 capsules

Capsule	12	11	10	9	8	7	6	5	4	3	2	1
Relative, %	5.3	10.1	2.5	3.8	3.8	2.4	4.2	3.9	4.0	3.0	3.0	4.3
Absolute, °C	46	125	30	39	45	33	45	40	41	36	32	40

#### 4. CONCLUSION

The temperature-uncertainty quantification uses nine inputs to the thermal model based on potential importance to calculated fuel-temperature uncertainties in the twelve AGR-3/4 capsules. This resulted from a combination of input uncertainties and sensitivities for fuel temperature. Expert judgment is used as a basis to specify the uncertainty range for select inputs. This also takes into account the events that occurred during irradiation, which can impact input

uncertainties. Additionally, AGR-3/4 PIE dimensional measurements were used to estimate the end-of-irradiation sizes for the four gas gaps, which led to a substantial reduction in gas gap size uncertainties for all capsules. The sensitivity analysis performed went beyond the traditional local sensitivity. Using an interpolation scheme over the input parameter domain, the analysis obtains time dependent sensitivity over the test campaign duration. This allows computation of uncertainty for the calculated fuel temperatures for each capsule and each time step over the entire irradiation period.

Forward propagation of model parameter uncertainties is used to quantify the parameter uncertainty of the calculated temperatures. Model form uncertainties (or model bias) are also included in the overall uncertainty. This model bias is based on the average of TC residuals during the first three ATR cycles when the TCs were more reliable. For the majority of capsules, thermal model results match well with thermocouple temperatures, indicating good prediction performance. Measures taken in thermal modeling for uncertainty reduction led to low fuel-temperature uncertainty in all AGR-3/4 capsules except Capsule 11, for which the model bias remains high.

Overall temperature uncertainty is calculated by combining input-parameter and model-form uncertainties. Relative uncertainties for Capsules 1–10 and 12 range from 2.4 to 5.3%, with Capsule 11 having the highest relative uncertainty at 10.1%. Absolute uncertainties for Capsules 1–10 and 12 range from 30–46°C, with Capsule 11 having the highest average absolute uncertainty of 125°C.

## 5. ACKNOWLEDGMENT

This work was supported and funded by the U.S. Department of Energy, NGNP Program, Idaho Operations Office Contract DE-AC07-05ID14517.

## 6. REFERENCES

- [1] Idaho National Laboratory, “Technical Program Plan for INL Advanced Reactor Technologies Technology Development Office/Advanced Gas Reactor Fuel Development and Qualification Program,” PLN-3636, Rev. 6, Idaho National Laboratory, (2017).
- [2] B. P. Collin, *AGR-3/4 Irradiation Test Final As-Run Report*, INL/EXT-15-35550, Rev. 1, Idaho National Laboratory, 2016.
- [3] J. W. Sterbentz, “JMOCUP As-Run Daily Physics Depletion Calculation for the AGR-3/4 TRISO Particle Experiment in ATR Northeast Flux Trap,” ECAR-2753, Rev 1, Idaho National Laboratory, 2015.
- [4] G. L. Hawkes, J. W. Sterbentz, J. T. Maki, and B. T. Pham, “Thermal Predictions of the AGR-3/4 Experiment Using Post Irradiation Examination Measured Time Varying Gas Gaps,” *Nuclear Engineering and Radiation Science* 3.1, July 2017.
- [5] B.T Pham, G. L. Hawkes, and J. J. Einerson, “Improving Thermal Model Prediction through Statistical Analysis of Irradiation and Post Irradiation Data from AGR Experiments,” *Nuclear Engineering and Design* 271 (2014), pp. 209–216.

- [6] B. T. Pham, G. L. Hawkes, and J. J. Einerson, “Uncertainty Quantification of Calculated Temperatures for Advanced Gas Reactor Fuel Irradiation Experiments,” *Nuclear Technology* 196 (November 2016), pp. 396–407.
- [7] G. L. Hawkes, J. W. Sterbentz, and B. T. Pham, “Sensitivity Evaluation of the AGR- 3/4 Experiment Thermal Model Irradiated in the Advanced Test Reactor,” *Proceedings of the International Mechanical Engineering Congress & Exposition Conference (ASME IMECE2015)*, Houston, Texas, November 2015, Paper 53544.
- [8] B. T. Pham, J. J. Einerson, G. L. Hawkes, N. J. Lybeck, and D. A. Petti, “Gap Size Uncertainty Quantification in Advanced Gas Reactor TRISO Fuel Irradiation Experiments,” *Proceedings of the 11th International Topical Meeting on Nuclear Reactor Thermal-Hydraulics (NUTHOS-11)*, Gyeongju, Korea, October 2016, Paper N11P1234.
- [9] J. M. Harp, “Analysis of Individual Compact Fission Product Inventory and Burnup for the AGR 1 TRISO Experiment using Gamma Spectrometry,” ECAR-1682, Rev. 3, Idaho National Laboratory, 2014.